RSC Advances

ROYAL SOCIETY OF CHEMISTRY

www.rsc.org/advances

Biodegrade polymeric gene delivering nanoscale hybrid micelles enhance suppression effect of LRIG1 in breast cancer

Abstract

To increase the incorporation efficiency and improve the release kinetics of the LRIG1 gene from monomethoxy-poly(ethylene glycol)–poly(L-lactic acid) (MPEG-PLLA) micelles, a flexible method for the fabrication of N-(2,3-Dioleoyloxy-1-propyl)trimethylammonium methyl sulfate (DOTAP)-embedded MPEG-PLLA (MPDT) nanoscale hybrid micelles was developed. The MPDT nanoscale hybrid micelles produced according to the optimal formulation were spherical in shape when observed by transmission electron microscopy (TEM), with a mean particle size of 23.5±2.6 nm, which increased to 32.73±3.4 nm after binding the plasmid. Compared with PEI25K, MPDT nanoscale hybrid micelles exhibited higher transfection efficiency and lower cytotoxicity. We also used MPDT nanoscale hybrid micelles to deliver the LRIG1 gene to treat breast cancer. MPDT delivered the LRIG1 gene (MPDT/LRIG1) and inhibited tumor cell proliferation, reducing the growth of 4T1 breast cancer cells *in vitro*. *In vivo* studies show that MPDT nanoscale hybrid micelles injected through the tail vein were able to deliver the LRIG1 gene efficiently and inhibited the growth of 4T1 breast cancer cells. These results indicate that MPDT nanoscale hybrid micelles delivering LRIG1 gene might be valuable in treating breast cancer in humans.

Keywords: gene therapy; suppression; breast cancer; LRIG1; nanoscale hybrid micelles

1. Introduction

Over the past 20 years, breast cancer has been identified as one of the most common types of cancer in women, and the number of breast cancer patients has increased consistently in most countries over the same period of time [1]. Although much progress has been made in breast cancer therapy, the 5-year survival rate of women with this cancer has not improved substantially [2]. Thus, finding novel therapeutic approaches is essential. Since 1990, clinicians have considered gene therapy a promising form of cancer treatment, and it was successfully applied in the treatment of two metastatic melanoma patients in 2006 [3, 4]. Leucine-rich repeats and immunoglobulin-like domains of protein 1 (LRIG1) can modulate the expression of epidermal growth factor receptor (EGFR) and its downstream signaling pathway, the phosphatidylinositol-3-kinase (PI3K)/AKT [5, 6]. Prior studies have found that this function of LRIG1 may allow it to act as a cancer suppressor gene [7, 8]. The existence of a feed-forward regulatory loop in breast tumor cells in which aberrant ErbB2 signaling suppresses LRIG1 protein levels results in ErbB2 overexpression [9]. An increasing amount of data suggests that treating cancer by delivering the LRIG1 gene is a highly relevant therapeutic strategy.

There are two common types of carriers for gene delivery: viral and non-viral vectors [10]. Although viral vectors have high transfection efficiency, they result in

many side effects, representing are a critical barrier to their use in therapy [11-13]. After the failure of several attempts at clinical gene therapy due to severe side effects caused by the viral vectors [14, 15], safety is of the utmost importance when considering the implementation of an advanced gene delivery system. Compared to viral vectors, non-viral vectors possess significant advantages such as safety, cost, and lack of restraint on the size of DNA to be delivered [15, 16]. Reduced pathogenicity and lack of capacity for insertional mutagenesis are two clear safety advantages of non-viral over viral vectors [10, 11].

Nanotechnology is a quickly developing field that is attracting attention as a possible method of drug delivery and cancer gene therapy [17-19], an important step in developing bio-drugs [20, 21]. Paclitaxel delivered by MPEG-PLLA micelles for treating advanced malignancies in the clinic achieved substantial antitumor efficacy in cancer patients, with reduced levels of hypersensitivity reactions and fluid retention [22, 23]. An amphiphilic block copolymer composed of hydrophobic and hydrophilic segments has the tendency to self-assemble into core–shell type colloidal carriers in a selective solvent. PEG has been used to improve the solubility and steric stability of many gene delivery systems, including micelles and liposomes [24, 25]. Bioinert water-compatible polymers can increase the circulation time by coating the delivery system, and they can also contribute to steric stabilization of the delivery vehicle against undesirable aggregation and non-specific electrostatic interactions with the surroundings [25].

Many carriers, including biodegradable micelles, were tested as vehicles for gene delivery. Cell-penetrating peptide-modified MPEG-PLA micelles for systemic gene

delivery were synthesized, and these micelles did not induce significant cytotoxicity [12, 14]. Another cationic lipid-assisted and hyper-branched PEI-grafted PEG-PLA nanoparticle was developed to transfer siRNA [25]. The use of polymeric micelles for intravenous delivery of functional genes holds much promise as an effective therapy for breast cancer. PEI is a class of cationic polymers with abundant positive surface charges, and it have been increasingly proposed as a safe viral vectors for their potential advantages [26]. However, PEI has the shortcoming of inducing obvious increases in hemolysis and aggregation of erythrocytes. Moreover, cytotoxicity increases with its transfection efficiency. DOTAP, the most widely used cationic lipid, is efficient in both *in vitro* and *in vivo* applications due to its high transfection efficiency and low toxicity [27]. Moreover, several scientists demonstrated its ability to complex plasmid DNA and the potent immunological adjuvant effect of DOTAP liposomes on dendritic cells [28, 29].

To develop a safe and efficient gene carrier, we developed a novel gene carrier by modifying the MPEG-PLLA matrix the cationic lipid DOTAP to improve the incorporation efficiency of the micelles. And then the modified MPEG-PLLA micelles by DOTAP were used to to deliver the anticancer bio-drug LRIG1 (MPDT nanoscale hybrid micelles), and to treat breast cancer *in vitro* and *in vivo* with the goals of improving water solubility, reducing systemic toxicity and targeting cargos to the cancer site. Our results show that it is possible to treat breast cancer through transfection of LRIG1 with an MPDT carrier.

2. Experimental

2.1. Materials

Monomethoxy poly(ethylene glycol) (MPEG, M_n=2000) was obtained from Fluka (USA), and N-(2,3-Dioleoyloxy-1-propyl)trimethylammonium methyl sulfate (DOTAP), branched polyethylenimine (MW=25000, PEI25K stannous), octanoate ($Sn(Oct)_2$), Dulbecco's modified Eagle's medium (DMEM), and 3-(4,5-dimethylthiazol-2-yl)-2,5-diphenyl tetrazolium bromide (MTT) were supplied by Sigma-Aldrich Co. LLC. (USA). L-lactide was supplied by Guangshui National Chemical Co.(Guangdong, China). The plasmids expressing LRIG1 were constructed as previously reported [7, 8]. The pcDNA3.1 (Invitrogen, San Diego, CA) plasmid (pEP) without LRIG1 was used as an empty carrier. All the plasmids were purified using an EndoFree plasmid Giga kit (Qiagen, Chatsworth, CA).

BALB/c mice (18±2 g) used in this study were purchased from the Laboratory Animal Center of Sichuan University (Chengdu, China). The mice were housed at a temperature of 20-22 °C, with relative humidity of 50-60%. They were maintained with free access to food and water under a 12 h light-dark cycle. All animal care and experimental procedures were conducted in strict accordance with the guidelines of the Institutional Animal Care and Use Committee (IACUC).

4T1 cells were purchased from the American Type Culture Collection (ATCC, USA). The cells were grown in DMEM supplemented with 10% fetal bovine serum (FBS, Gbico, USA), incubated at 37 °C in a humidified incubator with a 5% CO_2 atmosphere.

2.2. Synthesis of MPEG-PLLA copolymer and preparation of MPDT nanoscale

hybrid micelles

The MPEG-PLLA copolymer was prepared using ring-opening polymerization as reported previously [22, 23]. Briefly, MPEG (5.0 g) was melted in a dry, nitrogen-purged three-neck flask (50 mL) under a N_2 stream while being stirred. Anhydrous L-lactide (5.0 g) and $Sn(Oct)_2$ (0.5%) were then added under nitrogen. The mixture of reactants was maintained in a silicone oil bath at 125 °C while being stirred for 24 h. The crude product was dissolved in THF followed by precipitation in ice-cold diethyl ether, and the resultant precipitate was filtered. This process was performed in triplicate, and the resultant product was vacuum-dried at ambient temperature (yield 92%). To prepare DOTAP/MPEG-PLLA(MPDT) nanoscale hybrid micelles, 1 mg DOTAP and 9 mg MPEG-PLLA polymer were mixed and dissolved in methylene dichloride (KeLong Chemicals, Chengdu, China), followed by 1 h of rotary evaporation with heat. For micelle self-assembly, the lipid film was subsequently rehydrated in double-distilled water to a final concentration of 2 $mg \cdot mL^{-1}$. Finally, the micelles were stored at 4 °C until further use.

2.3. Characterization

1H NMR spectra of MPEG–PLLA copolymer (in $CDCl_3$) were recorded on Varian 400 spectrometer (Varian, USA) at 400 MHz using tetramethylsilane as an internal reference standard. The gel permeation chromatography (GPC) measurements were

conducted at 25 ^{o}C with a instrument of HPLC (Agilent 110, USA). A Zetasizer Nano ZS (Malvern determined, Worcestershire, UK) was used to determine particle size distribution and zeta potential of the MPDT nanoscale hybrid micelles. The temperature was maintained at 25 °C for the measurements. The data shown are the means of three test runs, and the morphology of MPDT nanoscale hybrid micelles was observed under a transmission electron microscope (TEM) (H-6009IV, Hitachi, Japan).

2.4. Gel retardation assay

The MPDT/plasmid complex micelles were mixed with 10% loading buffer, loaded into 1% agarose gels in TAE buffer and separated using electrophoresis at 120 V for 25 min. Then, 1 mg of plasmid was complexed with different ratios (1, 3, 5, 10, 15, 20 μg) of MPDT nanoscale hybrid micelles. The gel was stained with ethidium bromide (0.6 μg mL^{-1}), and the location of plasmid DNA was revealed using a UV XRS light (Bio-RAD ChemiDox, USA).

2.5. Transfection experiment

4T1 cells were seeded into 6-well plates (Becton-Dickinson, USA) at a density of 1×10^{5} cells per well in 2 mL of complete DMEM (containing 10% fetal bovine serum). After 24 h, the medium in each well was replaced with 1 mL fresh DMEM without

serum. Then, gene transfer complex micelles, including 4 μg of plasmids, were added to different amounts of the vector in fresh DMEM without serum. They were then mixed and incubated for 20 min at RT (the mass ratios of PEI25K/pGFP, DOTAP/pGFP and MPDT/pGFP were 2/1, 20/1 and 25/1, respectively). After 6 h of incubation, the medium was replaced with complete medium; after a further 24 h, the transfected cells were collected using a microscope, and the transfection efficiency was measured using a flow cytometer (Becton Dickinson, Franklin Lakes, NJ).

2.6. MTT assays

4T1 cells were plated at a density of 2×10^4 cells per well in 96-well plates and incubated for 24 hours at 37 °C in 100 μL of DMEM. Cell culture medium was replaced with 200 μL serum-free DMEM without antibiotics. Then, a series of different concentrations of the complex was added to the wells and incubated at 37 °C for 4 h. Next, cell viability was measured with an MTT test.

2.7. Anticancer activity of MPDT/LRIG1 nanoscale hybrid micelles on 4T1 cells *in vitro*

The 4T1 cells were plated in 96-well plates at a density of 2×10^4 cells per well in 100 μL of complete DMEM. After 24 h of incubation, the medium was replaced with

100 μL of fresh DMEM without serum, and the cells were exposed to normal saline (NS), MPDT nanoscale hybrid micelles (MPDT), MPDT/pEP or MPDT/LRIG1 hybrid micelles (1 μg DNA/20 μg MPDT) separately in DMEM without serum for 6 h. Then, the medium was replaced with normal DMEM for additional incubation. Finally, the result was evaluated using an MTT test.

Flow cytometry was performed for further investigation. The 4T1 cells were plated at a density of 1×10^5 /well in 6-well plates, and they were incubated with normal saline (NS), MPDT nanoscale hybrid micelles (MPDT), MPDT/pEP or MPDT/LRIG1 hybrid micelles (1 μg DNA/20 μg MPDT) for 48 hours. The cells in the 6-well plates were washed twice with 300 μL PBS, then detached with 300 μL trypsin/EDTA, and centrifuged 1500 rpm for 3 min to obtain the precipitate. The apoptosis of 4T1 cells was analyzed using a flow cytometer (ESP Elite, USA).

2.8. MPDT/LRIG1 nanoscale hybrid micelles for treating mice bearing 4T1 tumors *in vivo*

BALB/c mice were subcutaneously injected in the right flank with 100 μL of cell suspension containing 4×10^5 4T1 cells. When the mean tumor diameter was 6 mm, the mice were numbered and randomly divided into 4 groups, and they were injected through the tail vein with 9 dosages of MPDT/LRIG1 hybrid micelles (125 μg/5 μg), MPDT/pEP hybrid micelles (125 μg/5 μg), MPDT nanoscale hybrid micelles (125 μg)

or normal saline (control). The tumor volume was recorded every day. All mice were euthanized when the tumor size was greater than 15 mm in the control group or when the mice in the control group were noticeably ill; immediately after euthanasia, their tumors were dissected, weighed, and analyzed.

2.9. Histological analysis

2.9.1. CD31

Tumors were fixed for 24 h in 4% paraformaldehyde in PBS. Tissues were dehydrated, embedded, cut into sections 3-5 μm thick and stained with hematoxylin and eosin.

Tumor microvessel density was estimated using immunofluorescent analysis of neovascularization in tumor tissue. The frozen sections of tumors were immersed in acetone, washed, incubated and stained with rat anti-mouse CD31 polyclonal antibody (BD Pharmingen TM, USA). The tissue samples were then washed with PBS and incubated with a FITC-conjugated secondary antibody (Abcam, USA). Microvessel density was calculated by counting the number of microvessels per high-power field in the sections under a fluorescence microscope.

2.9.2. Ki67

To quantify the Ki67 protein expression, the tumor tissues sections were stained for Ki67 using the labeled streptavidin–biotin method. The primary antibody was rat anti-mouse monoclonal anti-Ki67 (Gene Tech), and the secondary antibody was

biotinylated goat anti-rat immunoglobulin (BD Biosciences Pharmingen). For this assay, 5 tumors per group were stained, and 5 random sections were counted; the Ki67 labeling index (LI) was calculated as the number of Ki67-positive cells/total number of cells counted × 100% under ×200 magnification.

2.10. Statistical analysis

All the data are expressed as the mean with 95% confidence intervals. Statistical analyses were performed using one-way analysis of variance, and the results are expressed as the mean ± standard deviation. For all results, $P<0.05$ was considered statistically significant.

3. Results

3.1. Synthesis and characterization of MPDT nanoscale hybrid micelles

“embed Fig. 1”

Recently, we synthetized a novel non-viral gene delivery system based on DOTAP and MPEG-PLLA that may be a gene vector with low cytotoxicity and high transfection efficacy. The preparation schemes for MPDT and MPEG-PLLA micelles are presented in Fig. 1. DOTAP and MPEG-PLLA polymer were mixed and dissolved in methylene dichloride, followed by 1 h of rotary evaporation with heat. They can self-assemble into micelles and form a core–shell structure in the water because both MPEG-PLLA and DOTAP are amphiphilic. In this structure, DOTAP heads are present on the surface of MPDT nanoscale hybrid micelles, and the electrostatic attraction can deliver DNA on the surface.

The ^{1}H-NMR of MPEG-PLLA was showed in Fig. 2B. the sharp peaks at 3.60 and 3.38 ppm are attributed to methylene protons of $–CH_2CH_2O–$ and $–OCH_3$ end groups in PEG blocks, respectively. Peaks at 5.20 and 1.54 were assigned to methyl group and methylene protons of $–CH_3$, and –CH– in PLA units, respectively. The GPC curve of MPEG-PLLA was showed in Fig. 3B. Only asingle peak existed in Fig. 3B, which indicated the mono-distribution of molecular weight. The macromolecular weight distribution (polydispersity, PDI, Mw/Mn) was 1.20.

"embed Fig. 2"

We characterized the MPDT nanoscale hybrid micelles as shown in Fig. 3. MPEG-PLLA micelles were monodisperse with a mean particle size of 23.5±2.6 nm, and after binding the plasmids, the micelles had a mean particle size of 32.73±3.4 nm. As shown in the TEM image, we can observe that MPDT nanoscale hybrid micelles are spherical (Fig. 3C). An agarose gel retardation assay was performed to assess the capacity of MPDT to carry DNA. The results are shown in Fig. 3D. Based on this result, we can say that completely retarded DNA migration was achieved when the N/P ratio ≥8, which suggests that MPDT nanoscale hybrid micelles can efficiently deliver genes to cells. The aqueous solutions of NS, MPDT and MPDT/LRIG1 are shown in Fig. 3E. In addition, the MPDT nanoscale hybrid micelles could be stored at 25 °C for one month without aggregating.

"embed Fig. 3"

Next, the transfection efficiency and cytotoxicity of MPDT nanoscale hybrid

micelles was compared with DOTAP and PEI25K *in vitro*; Fig. 4A and Fig. 4B show the transfection ability of MPDT with a pGFP-based reporter plasmid. MPDT nanoscale hybrid micelles have higher transfection efficiency and lower cytotoxicity than PEI25K. Fig. 4E shows that PEI25K induced substantial toxicity, with an IC_{50}<10 μg mL^{-1}. The MPDT nanoscale hybrid micelles were much less toxic, and their IC_{50} values were greater than 1 mg mL^{-1}. Fig. 4F shows that 4T1 cells can be transfected using MPDT/pGFP hybrid micelles. The transfection efficiency of MPDT on 4T1 cells was 36±2.5%, compared with 30±6.9% for DOTAP and 31±3.2% for PEI25K. Therefore, we can say that MPDT nanoscale hybrid micelles may be an effective and safe gene vector.

"embed Fig. 4"

3.2. Antitumor activity *in vitro*

In the MPDT/LRIG1 group (Fig. 5A), 40±3.6% of the cancer cells were observed to be apoptotic, compared with 17±2.1% for the MPDT/pEP hybridmicelles and 11±1.6% for the MPDT nanoscale hybrid micelles. After treatment for 24 h, MPDT/LRIG1 hybrid micelles (25 μg MPDT/5 μg LRIG1), MPDT/pEP hybrid micelles (25 μg MPDT/5 μg pEP), and MPDT nanoscale hybrid micelles (25 μg) caused 71±4.1%, 25±3.5%, and 5.2±1.3% (shown in Fig. 5B) inhibition of 4T1 cell growth, respectively. From this result, we can infer that MPDT nanoscale hybrid micelles can deliver the LRIG1 gene into cells *in vitro* and efficiently inhibit tumor cell proliferation.

"embed Fig. 5"

3.3. Antitumor activity *in vivo*

The ability to effectively express LRIG1 *in vivo* using MPDT nanoscale hybrid micelles was demonstrated in a hypodermic tumor model. Fig. 6 shows representative images of a diminution in size of 4T1 breast cancers in each treatment group (Fig. 6A). The tumor tissues in each group were harvested and weighed, and the results are illustrated in Fig. 6B. The tumor weight in the MPDT/LRIG1 complex group was 1.16±0.32 g, compared with 2.4±0.64 g in the control group, 2.33±0.25 g in mice treated with MPDT nanoscale hybrid micelles, and 1.73±0.61 g in mice treated with MPDT/PEP complex micelles. Compared with the control group, the MPDT/LRIG1 complex micelles caused a statistically significant reduction in tumor weight ($P< 0.01$). As shown in Fig. 6C, there was also a statistically significant decrease in the tumor volume in the MPDT/LRIG1 mice compared with the other groups. The tumor volume in the mice treated with MPDT/LRIG1 hybrid micelles was 1564.3±97.4 mm^3, compared with 2550.2±62.1 mm^3 in the control group ($P< 0.01$), 2388.6±118.9 mm^3 in the MPDT nanomicelle group, and 2293 ±102.2 mm^3 in the MPDT/pEP hybrid nanomicelle group. Furthermore, an increase in the life span of the each group of mice was observed. Compared with the mice in the NS group, MPDT hybrid micelles and MPDT/pEP hybrid micelles prolonged the survival time of tumor-bearing mice (Fig. 6D). Therefore, the tumor growth in the mice treated with MPDT/LRIG1 complex micelles was obviously suppressed and prolongs the survival of mice.

"embed Fig. 6"

A subdermal assay was conducted to further study the mechanism associated with

the antitumor activity of MPDT/LRIG1 complex micelles *in vivo*. Sections of tumors from mice in each group were stained for CD31 to determine the microvessel density (MVD) as a measurement of tumor angiogenesis (Fig. 7), and the results suggest that inhibiting tumor cell proliferation might be one of the most important mechanisms of this study. As shown in Fig. 8, we examined the effects of complex micelles on the proliferation of tumor cells using immunohistochemical staining for Ki67. The tumor tissues in the group treated with MPDT/LRIG1 hybrid micelles showed fewer Ki67-positive cells and weaker Ki67 immunoreactivity than the mice in the NS, MPDT hybrid nanomicelle, and MPDT complex groups. As shown in Fig. 8E, the Ki67 LI in MPDT/LRIG1 hybrid nanomicelle group was 24.91±1.98%, while the LI was 78.83±3.81% in the NS group, 54.16±2.85% in the MPDT complex group, and 46.33±5.32% in the MPDT/pEP hybrid nanomicelle group.

"embed Fig. 7"

4. Discussion

Cancer is a major public health concern in the modern world; more than 25% of the deaths in the United States are caused by cancer. Today, treatment of cancer is one of the most important scientific issues, making the development of an effective cancer therapy method highly desirable [18]. Many functional genes have been identified in association with various tumor types, but the lack of safe and efficient gene delivery technologies has restricted the application of gene therapy in the clinic [13, 15]. Viral

vectors were used as carriers for a large proportion of gene delivery and expression studies *in vivo* in the early stages of clinical research [30, 31]. Several cancer gene therapy applications seemed promising in early-phase clinical trials with conditionally replicating viruses. Although viral vectors are among the most efficient gene vectors, in 1999, Jesse Gelsinger died from experimental adenoviral gene therapy. After that, the safety of viral vectors received additional scrutiny. Non-viral gene vectors have great advantages over viral vectors, particularly in terms of safety [32, 33]. Currently, there are many non-viral vectors being tested in clinical trials of cancer gene therapy, but the non-viral gene delivery methods are limited by low efficiency [34].

"embed Fig. 8"

In this paper, the DOTAP was incorporated into the MPEG-PLLA matrix to prepare DOTAP-modified MPEG-PLLA (MPDT). And then biodegradable self-assembled MPDT nanoscale hybrid micelles was synthesized as a gene delivery vector with potential application in gene delivery and used these micelles to deliver the LRIG1 gene to treat 4T1 breast cancer. Although the introduction of a cationic compound into the PLA-PEG matrix has previously been reported to improve the transfection efficiency and cytotoxicity [24], no studies have to our knowledge reported on the DOTAP-modification of MPEG-PLLA micelles loaded with LRIG1 gene. Our results suggest that MPDT has lower toxicity and higher transfection efficiency than PEI25K, which is the current gold standard, indicating the MPDT nanoscale hybrid micelles as a new non-viral gene vector. Furthermore, the MPDT-delivered LRIG1 gene (MPDT/LRIG1) was observed to inhibit the

proliferation of 4T1 breast cancer cells *in vitro*. More importantly, MPDT/LRIG1 inhibited the metastasis of 4T1 breast cancer *in vivo*.

DOTAP has been widely used in gene-delivery systems, and drugs containing DOTAP have been approved. DOTAP can generate a positive charge and produces high cytotoxicity [35]. Since the beginning of cancer gene therapy, DOTAP cationic liposomes have become a mature system that is capable of transferring RNA and plasmids and has been applied in clinical situations. DOTAP cationic liposomes have also shown antitumor efficacy in peritoneal disseminated tumors [33].

Biodegradable MPEG-PLLA self-assembled micelles have potential applications in gene delivery. There are two mechanisms for their adsorption. The first is by adsorbing DNA onto the surface of cationic MPEG-PLLA micelles via electrostatic interaction. Binding the DNA via electrostatic interaction is simple, but this method requires modification of the vector [33, 37]. Therefore, a more convenient method is needed and is now under development. The other mechanism involves encapsulating DNA into micelles by nano-fabrication [34, 36, 37]. For this method, the micelle structures usually encapsulate DNA molecules directly with violent stirring in organic solvents, which often leads to low entrapment efficiency and DNA damage. We aimed to design a simple physical modification of MPEG-PLLA micelles for gene delivery.

As a normal drug delivery vector, MPEG-PLLA micelles can carry a large drug load. In water, this polymer automatically forms a core-shell structure through one-step self-assembly [22, 23]. However, to prepare a gene vector, MPEG-PLLA is usually chemically modified with certain cationic hybrid micelles, such as DOTAP. In

a previous study, we improved the water solubility of deguelin by using biodegradable nanoparticles. Then, we designed and prepared MPEG-PLLA and DOTAP: MPEG-PLLA micelles could embed the DOTAP molecule through self-assembly in water. The surface charge of DOTAP affects the cellular uptake and tissue absorption of nanoparticles and can be retained with reduced toxicity [17, 36]. Our result indicated that the PEI25K and DOTAP micelles were more toxic than MPDT nanoscale hybrid micelles, which have high capacities for DNA adsorption and delivery. MPDT nanoscale hybrid micelles with N/P ratio equal to 10 were used for further in vitro and in vivo test. To our knowledge, this is the first report of a self-assembling vector composed of MPEG-PLLA and DOTAP. We also hope that these micelles will represent a new method of gene delivery.

EGFR and E-cadherin are known to co-localize upon cell-cell contact. E-cadherin protein levels increase five-fold at cell confluence, and EGFR mRNA and protein levels remain constant, but their tyrosine kinase activity is reduced [38]. The mechanism by which EGFR activation decreases at cell confluence is not well understood. Speculation about the causes of this drop in EGFR phosphorylation involves an inhibitory interaction between EGFR and E-cadherin, but to our knowledge, there are no data to support this causal relationship [39, 40]. The endogenous EGFR inhibitory molecule LRIG1 is also recruited to the complex at cell confluence, and it is required for density-dependent growth inhibition [8].

All tissues can express LRIG1, and both endogenous and synthetic LRIG1 have been confirmed to be plasma membrane-bound by cell surface

biotinylation/precipitation, laser microscopy and confocal immunofluorescence [41-43]. Previous research suggests that LRIG1 blocks EGFR activation through two possible mechanisms. One is that the LRIG1 transcript and protein are known to be upregulated after EGF stimulation. This is thought to be a negative feedback mechanism in which LRIG1 associates with all four EGFR analogues, and both proteins are subsequently ubiquitinated by ubiquitin ligases [39, 44, 45]. LRIG1 has been postulated to bind EGFR in a monomeric 'attenuated' state [46, 47]. The resulting LRIG1 with the intracellular domain deleted, but including the c-Cbl E3 ubiquitin ligase-binding domain, still inhibits EGFR activity without physical downregulation of the protein and without competing for EGF binding [7, 9]. The latter occurs in density-dependent growth inhibition: no downregulation of the EGFR protein itself occurs, but a dramatic fall in EGFR activity is observed at cell-cell contact along with LRIG1 expression [39, 40]. This influenced our decision to deliver LRIG1 to tumors using MPDT nanoscale hybrid micelles and produce anti-tumor effects by inhibiting tumor cell proliferation. In this study, the group of mice treated with MPDT/LRIG1 complex micelles exhibited much lower tumor weights. We believe that the MPDT nanoscale hybrid micelles successfully delivered the LRIG1 gene to breast tumor tissues and inhibited tumor cell proliferation.

5. Conclusion

We synthesized novel biodegradable DOTAP and MPEG-PLLA micelles for gene

delivery. The micelles were demonstrated to be a novel gene vector with low toxicity and high transfection efficiency. The MPDT nanoscale hybrid micelles were synthesized by self-assembly. The particle size and TEM image of the micelles indicated that they were stable and soluble. Furthermore, DOTAP/MPEG-PLLA micelles, which delivered LRIG1 genes, efficiently inhibited the growth of 4T1 breast carcinomas.

Declaration of financial disclosure

We have no conflicts of interest to declare.

References

[1] R. Siegel, D. Naishadham, A. Jemal, Cancer statistics, CA. Cancer. J. Clin 63 (2013) 11-30.

[2] R. Machii, K. Saika, Estimated disability-adjusted life year (DALY) in Asia in GLOBOCAN 2008, Jpn. J. Clin. Oncol. 43 (2013) 846-847.

[3] R.A. Morgan, M.E. Dudley, J.R. Wunderlich, M.S. Hughes, J.C. Yang, R.M. Sherry, R.E. Royal, S.L. Topalian, U.S. Kammula, N.P. Restifo, Cancer regression in patients after transfer of genetically engineered lymphocytes, Science. 314 (2006) 126-12.

[4] IM. Verma, N. Somia, Gene therapy-promises problems and prospects, Nature.

389 (1997) 239-242.

[5] L.C. Bai, D. McEachern, C.Y. Yang, J.F. Lu, H.Y. Sun, S.M. Wang, LRIG1 modulates cancer cell sensitivity to Smac mimetics by egulating TNF α expression and receptor tyrosine kinase signaling, Cancer. Res. 75 (2012) 1229-1238.

[6] L. Lu, V.H. Teixeira, Z. Yuan, T.A. Graham, D. Endesfelder, K. Kolluri, N. Al-Juffali, N. Hamilton, A.G. Nicholson, M. Falzon, LRIG1 regulates cadherin-dependent contact inhibition directing epithelial homeostasis and pre-invasive squamous cell carcinoma development, J. Pathol. 229 (2013) 608-620.

[7] F. Li, Z.Q. Ye, D.S. Guo, W.M. Yang, Suppression of bladder cancer cell tumorigenicity in an athymic mouse model by adenoviral vector-mediated transfer of LRIG1, Oncol. Rep. 26 (2011) 439-446.

[8] I. Ljuslinder, I. Golovleva, R. Palmqvist, A. Oberg, R. Stenling, Y. Jonsson, H. Hedman, R. Henriksson, B. Malmer, LRIG1 expression in colorectal cancer, Acta. Oncol. 46 (2007) 1118-1122.

[9] J.K. Miller, D.L. Shattuck, E.Q. Ingalla, L. Yen, A.D. Borowsky, L.J. Young, R.D. Cardiff, K.L.III. Carraway, C. Sweeney, Suppression of the negative regulator LRIG1 contributes to ErbB2 overexpression in breast cancer. Cancer. Res. 68 (2008) 8286-94.

[10] R.J. Brandwijk, A.W. Griffioen, V.L. Thijssen, Targeted gene-delivery strategies for angiostatic cancer treatment, Trends. Mol. Med. 13 (2007) 200-209.

[11] D.J. Glover, H.J. Lipps, D.A. Towards safe non-viral therapeutic gene expression in humans, Nat. Rev. Genet. 6 (2005) 299-U29.

[12] W. L, Q. Sun, J. Wan, Z.J. She, X.G. Jiang, Cationic albumin–conjugated pegylated nanoparticles allow gene delivery into brain tumors via intravenous administration, Cancer. Res. 66 (2006) 1878-87.

[13] R.R. Fan, X.H. Deng, L.X. Zhou, X. Gao, M. Fan, Y.L. Wang, G. Guo, Injectable thermosensitive hydrogel composite with surface-functionalized calcium phosphate as raw materials, Int. J. Nanomed. 9 (2014) 615–626

[14] C.Y. Wang, S. Ravi, G.V. Martinez, V. Chinnasamy, P. Raulji, M. Howell, Y. Davis, J. Mallela, M.S. Seehra, S. Mohapatra, Dual-purpose magnetic micelles for MRI and gene delivery, J. Control. Release. 163 (2012) 82-92.

[15] E. Marshall, Clinical trials-Gene therapy death prompts review of adenovirus vector, Science. 286 (1999) 2244-2245.

[16] X.H. Wang, L.Y. Deng, X. Chen, H.Y. Pei, L.L. Cai, X. Zhao, Y.Q. Wei, L.J. Chen, Truncated bFGF-mediated cationic liposomal paclitaxel for tumor-targeted drug delivery: improved pharmacokinetics and biodistribution in tumor-bearing mice, J. Pharm. Sci. 100 (2011) 1196-1205.

[17] Y.L. Wang, G. Gang, H.F. Chen, X. Gao, R.R. Fan, D.M. Zhang, L.X. Zhou, Preparation and characterization of polylactide/poly(ε-caprolactone)-poly(ethylene glycol)-poly(ε-caprolactone) hybrid fiers for potential application in bone tissue engineering, Int. J. Nanomedicine. 9 (2014) 1991-2003.

[18]. L.L. De, J.C. Rea, L.D. Shea, Design of modular non-viral gene therapy vectors, Biomaterials. 27 (2006) 947-954.

[19] G. Guo, S.Z. Fu, L.X. Zhou, H. Liang, M. Fan, F. Luo, Z.Y. Qian, Y.Q. Wei, Preparation of curcumin loaded poly(ε-caprolactone)-poly(ethylene glycol)-poly(ε-caprolactone) nanofibers and their in vitro antitumor activity against Glioma 9L cells, Nanoscale 3 (2011) 3825-3832.

[20] X.Y. Li, Z.L. Zhang, J. Li, S. M. Sun, Y.H. Weng, H. Chen, Diclofenac/biodegradable polymer micelles for ocular applications, Nanoscale. 4 (2012) 4667-4673.

[21] R.R. Fan, Y.L. Wang, B. Han, Y.F. Luo, L.X. Zhou, X.R. Peng, M. Wua, Y. Zheng, G. Guo, Docetaxel load biodegradable porous microspheres for the treatment of colorectal peritoneal carcinomatosis, Int. J. Biol. Macromol. 69 (2014) 100-107.

[22] T.Y. Kim, D.W. Kim, J.Y. Chung, S.G. Shin, S.C. Kim, D.S. Heo, N.K. Kim, Y.J .Bang, Phase I and Pharmacokinetic Study of Genexol-PM, a CremophorFree, Polymeric Micelle-Formulated Paclitaxel, in Patients with Advanced Malignancies, Clin. Cancer. Res. 17 (2004) 3708-3716.

[23] S.W. Lee, M.H. Yun, S.W. Jeong, C.H. In, J.Y. Kim, M.H. Seo, C.M. Pai, S.O. Kim, Development of docetaxel-loaded intravenous formulation, Nanoxel-PM™ using polymer-based delivery system, J. Control. Release. 155 (2011) 262-271.

[24] C. Liu, Z. Chen, W. Yu, N. Zhang, Novel cationic 6-lauroxyhexyl lysinate modified poly(lactic acid)–poly(ethylene glycol) nanoparticles enhance gene transfection, J. Colloid. Interface. Sci. 354 (2011) 528-535.

[25] X.Z. Yang, S. Dou, T.M. Sun, C.Q. Mao, H.X. Wang, J. Wang, Systemic delivery of siRNA with cationic lipid assisted PEG-PLA nanoparticles for cancer therapy, J. Control. Release. 156 (2011) 203-11.

[26] K. Sun, J. Wang, J. Zhang, M. Hua, C. Liu, T. Chen, Dextran–g–PEI nanoparticles as a carrier for co-delivery of adriamycin and plasmid into osteosarcoma cells, Int. J. Biol. Macromol. 49 (2011) 173-180.

[27] D. Simberg, S. Weisman, Y. Talmon, Y. Barenholz, DOTAP (and other cationic lipids): chemistry, biophysics, and transfection, Crit. Rev. Ther. Drug. Carrier. Syst. 21(2004) 257-317.

[28] D.K. Jensen, L.B. Jensen, S. Koocheki, L. Bengtson, D. Cun, H.M. Nielsen, C. Foged, Design of an inhalable dry powder formulation of DOTAP-modified PLGA nanoparticles loaded with siRNA, J. Control. Release. 157 (2012) 141-148.

[29] M.C. Terp, F. Bauer, Y. Sugimoto, B. Yu, R.W. Brueggemeier, L.J. Lee, R.J. Lee, Differential efficacy of DOTAP enantiomers for siRNA delivery *in vitro*, Int. J. Pharm. 430 (2012) 328-334.

[30] C.E. Thomas, A. Ehrhardt, M.A. Kay, Progress and problems with the use of viral vectors for gene therapy, Nat. Rev. Genet. 4 (2003) 346-358.

[31] R.J. Yanez-Munoz, K.S. Balaggan, A.N. Mac, S.J. Howe, M. Schmidt, A.J. Smith, P. Buch, R.E. MacLaren, P.N. Anderson, S.E. Barker, Effective gene therapy with nonintegrating lentiviral vectors, Nat. Med. 12 (2006) 348-353.

[32] D. Doroud, A. Vatanara, F. Zahedifard, E. Gholami, R. Vahabpour, N.A. Rouholamini, S. Rafati, Cationic solid lipid nanoparticles loaded by cysteine

proteinase genes as a novel anti-leishmaniasis DNA vaccine delivery system: characterization and in vitro evaluations, J. Pharm. Pharm. Sci. 13 (2010) 320–335.

[33] M. Singh, M. Briones, G. Ott, D. O'Hagan, Cationic microparticles: A potent delivery system for DNA vaccines, Proc. Natl. Acad. Sci. U.S.A. 97 (2000) 811-816.

[34] S.K. Pandey, S.Ghosha, P.Maitib, C. Haldar, Therapeutic efficacy and toxicity of tamoxifen loaded PLA nanoparticles for breast cancer, Int. J. Biol. Macromol. 72 (2014) 309-319.

[35] D. Simberg, S. Weisman, Y. Talmon, Y. Barenholz, DOTAP (and other cationic lipids): Chemistry biophysics and transfection, Crit. Rev. Ther. Drug. Carrier. Syst. 21 (2004) 257-317.

[36] M.E. Davis, Z. Chen, D.M. Shin, Nanoparticle therapeutics: an emerging treatment modality for cancer, Nat. Rev. Drug. Discov. 7 (2008) 771-782.

[37] B. Gopalan, I. Ito, Branch, C. Stephens, J.A. Roth, R. Ramesh, Nanoparticle based systemic gene therapy for lung cancer: Molecular mechanisms and strategies to suppress nanoparticle-mediated inflammatory response, Technol. Cancer. Res. Treat. 3 (2004) 647-657.

[38] X.C. Qi, D.J. Xie, Q.F. Yan, Y.R. Wang, Y.X. Zhu, C. Qian, S.X. Yang, LRIG1 dictates the chemo-sensitivity of temozolomide (TMZ) in U251 glioblastoma cells via down-regulation of EGFR/topoisomerase-2/Bcl-2, Biochem. Bioph. Res. Co. 437 (2013) 565-572.

[39] M. Johansson, A. Oudin, K. Tiemann, A. Bernard, A. Golebiewska, O. Keunen, F. Fack, D. Stieber, B.F. Wang, H. Hedman, The soluble form of the tumor suppressor Lrig1 potently inhibits in vivo glioma growth irrespective of EGF receptor status, Neuro-Oncology. 15 (2013) 1200-1211.

[40] Q. Guo, J.W. Zhang, T.T. Liu, X.C. Wang, Intermediates in the refolding of urea-denatured-dimeric arginine kinase from Stichopus japonicus, Int. J. Biol. Macromol. 41 (2007) 521-528.

[41] F. Ye, Q.L. Gao, T.J. Xu, L. Zeng, Y.B. Ou, F. Mao, H.P. Wang, Y. He, B.F. Wang, Z.M. Yang, Upregulation of LRIG1 suppresses malignant glioma cell growth by attenuating EGFR activity, J. Neuro-Oncol. 94 (2009) 183-194.

[42] F. Mao, B.F. Wang, Q.G. Xiao, G.F. Xi, W. Sun, H.Q. Zhang, F. Ye, F. Wan, D.S. Guo, T. Lei, A role for LRIG1 in the regulation of malignant glioma aggressiveness, Int. J. Oncol. 42 (2013) 1081-1087.

[43] M. Nagata, T. Nakamura, C. Sotozono, T. Inatomi, N. Yokoi, S. Kinoshita, LRIG1 as a potential novel marker for neoplastic transformation in ocular surface squamous neoplasia, Plos. One. 9 (2014) e93164.

[44] X. Li, F. Qin, L. Yang, L.Q. Mo, L. Li, L.B. Hou, Sulfatide-containing lipid perflorooctylbromide nanoparticles as paclitaxel vehicles targeting breast carcinoma, Int. J. Nanomedicine. 9 (2014) 3971-3985.

[45] Y. Wang, E.J. Poulin, R.J. Coffey, LRIG1 is a triple threat: ERBB negative regulator intestinal stem cell marker and tumour suppressor, Brit. J. Cancer. 108 (2013) 1765-1770.

[46] R. Vivek, R. Thangam, V. Nipunbabua, T. Ponraj, S. Kannan, Oxaliplatin-chitosan nanoparticles induced intrinsic apoptotic signaling pathway: A "smart" drug delivery system to breast cancer cell therapy, Int. J. Nanomedicine. 65 (2014) 289-297.

[47] S. Muller, D. Lindquist, L. Kanter, C. Flores-Staino, R. Henriksson, H. Hedman, Expression of LRIG1 and LRIG3 correlates with human papillomavirus status and patient survival in cervical adenocarcinoma, S. Int J. Oncol. 42 (2013) 247-252.

Figure legends

Figure 1 Synthesis of DOTAP/MPEG-PLLA hybrid micelles. **A** Molecular structures

of DOTAP using in this study; **B** Synthesis scheme for MPDT hybrid micelles.

Figure 2 Preparation of MPEG-PLLA. A The synthesis scheme of MPEG-PLLA; B The ^{1}H-NMR curve of MPEG-PLLA.

Figure 3 Characterization of micelles. **A** Size distribution spectrum of MPDT before binding plasmids (a); Size distribution spectrum of MPDT after binding plasmids (b); B The GPC curve of MPEG-PLLA; **C** TEM image of MPDT after binding plasmids; **D** Gel retardation assay (PEI25K, DOTAP and MPDT); **E** Images of NS, MPDT and MPDT/LRIG1 dissolved in water.

Figure 4 Effects of transfection of 4T1 breast tumor cells *in vitro*. **A** Photograph of 4T1 cells transfected by MPDT/pEP in fluorescent light; **B** Photograph of 4T1 cells transfected by MPDT/pEP in fluorescent light; **C** Photograph of 4T1 cells transfected by MPDT/ LRIG1 in fluorescent light; **D** Photograph of 4T1 cells transfected by MPDT/ LRIG1 in fluorescent light; **E** Cell viability assay (MPDT, DOTAP and PEI25K); **F** *In vitro* transfection efficiency of MPDT, DOTAP and PEI25K.

Figure 5 Cytotoxicity studies of MPDT micelles on 4T1 cells. **A** Apoptosis measured by flow cytometric analysis; **B** Cytotoxicity evaluation of MPDT micelles on 4T1 cells *in vitro* by MTT assay. * $P<0.05$.

Figure 6 MPDT micelles inhibited growth in a subcutaneous model of 4T1 breast cancer. **A** Photographs of subcutaneous tissue bearing metastases of 4T1 breast cancer; **B** Weight of subcutaneous metastases of 4T1 breast carcinoma; **C** Tumor volume of 4T1 breast carcinoma; **D** Survival curves of mice. * $P<0.05$.

Figure 7 CD31 immunohistochemical staining of subdermal metastases of 4T1 breast carcinoma. **A** Control group; **B** MPDT micelle group; **C** MPDT/pEP complex group; **D** MPDT/LRIG1 complex group; **E** The MVD in each group. *$P<0.05$.

Figure 8 Ki67 immunohistochemical staining of subdermal metastases of 4T1 breast carcinoma. **A** Control group; **B** MPDT micelle group; **C** MPDT/pEP complex group; **D** MPDT/LRIG1 complex group; **E** Ki67 LI in each group. *$P<0.05$.

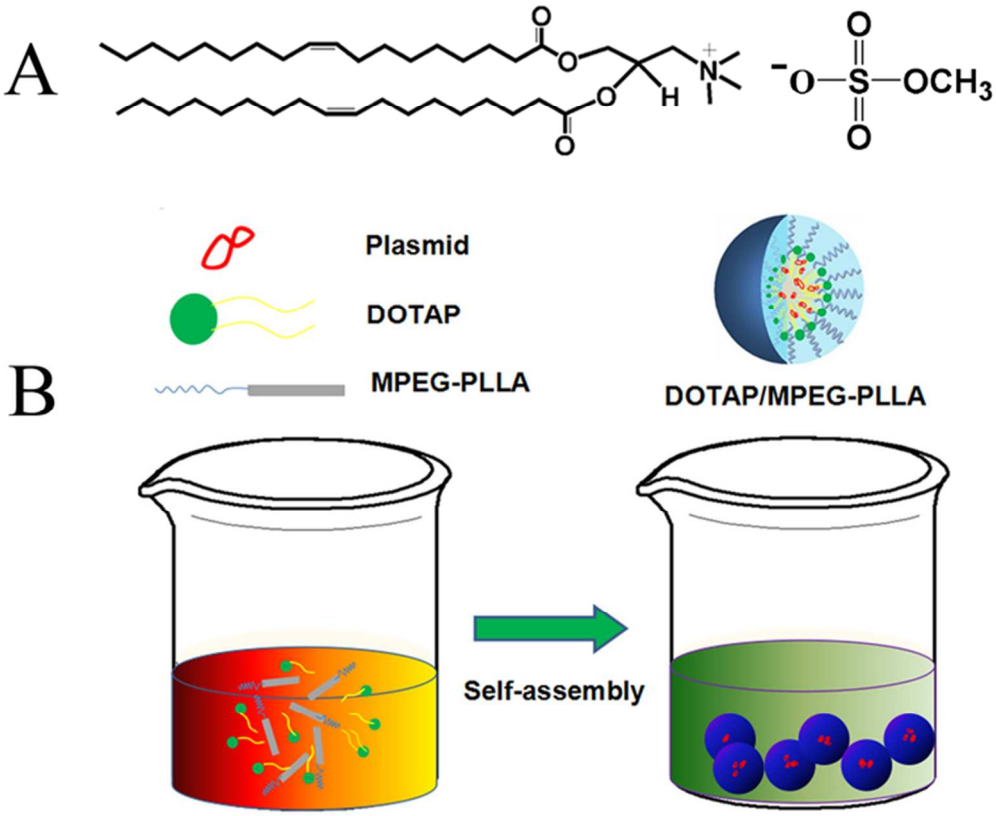

A biodegrade polymeric gene delivering nanoscale hybrid micelles enhance suppression effect of LRIG1 in breast cancer
64x52mm (300 x 300 DPI)

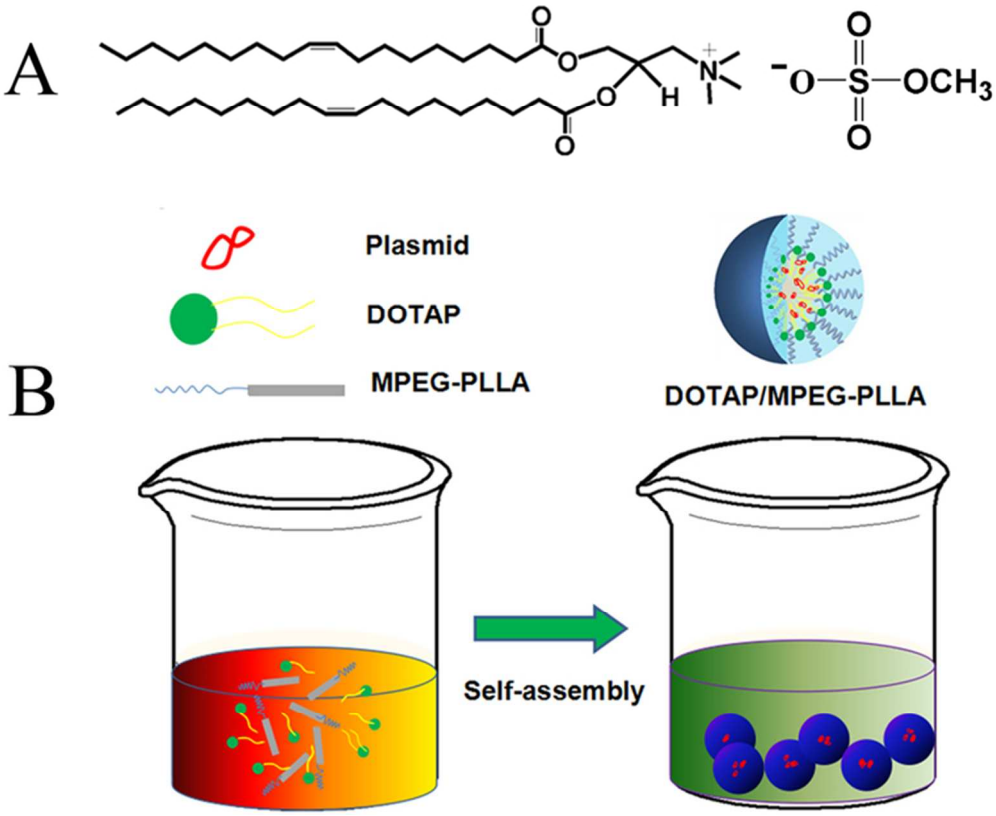

Figure 1 Synthesis of DOTAP/MPEG-PLLA hybrid micelles. A Molecular structures of DOTAP using in this study; B Synthesis scheme for MPDT hybrid micelles.
64x52mm (300 x 300 DPI)

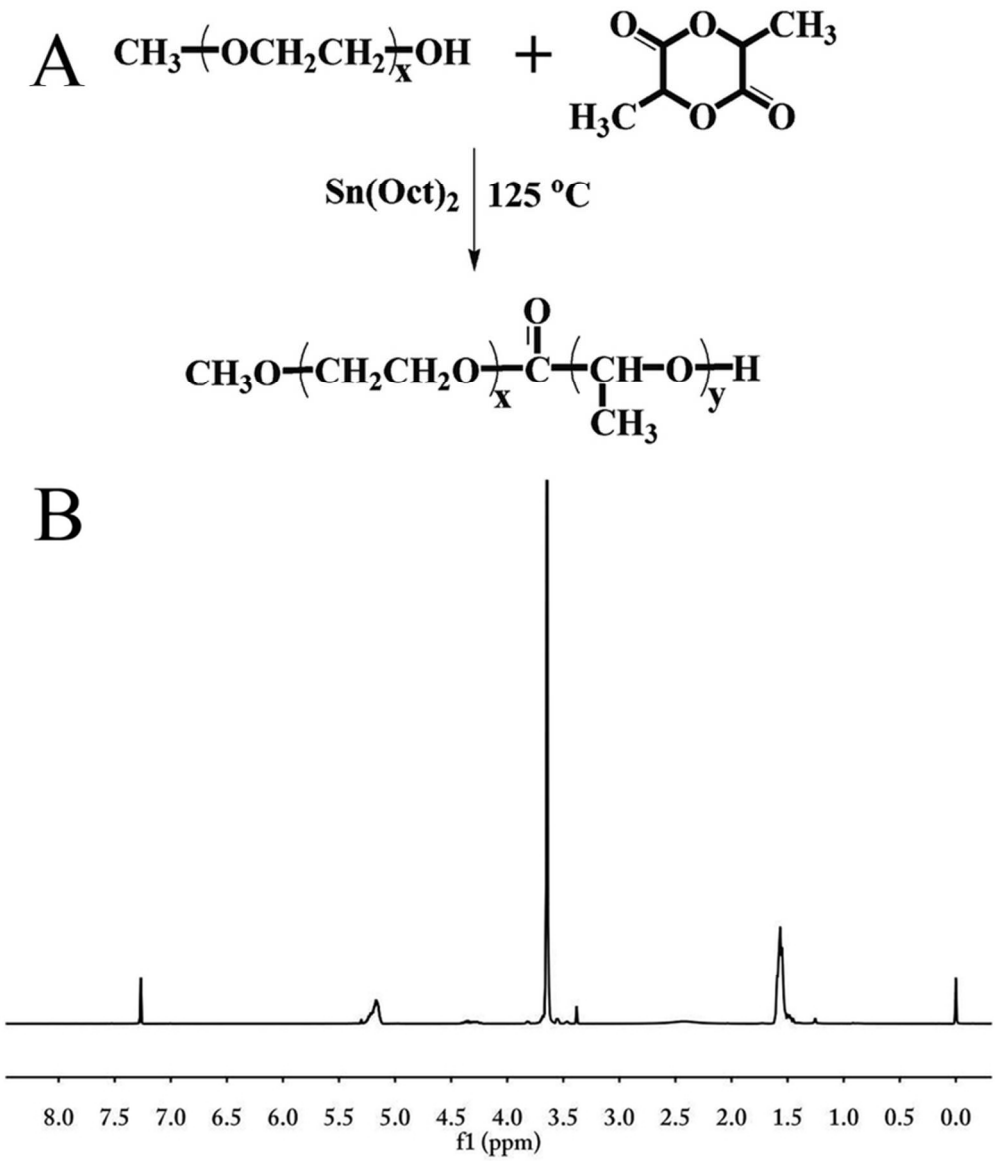

Figure 2 Preparation of MPEG-PLLA. A The synthesis scheme of MPEG-PLLA; B The 1H-NMR curve of MPEG-PLLA.
71x84mm (300 x 300 DPI)

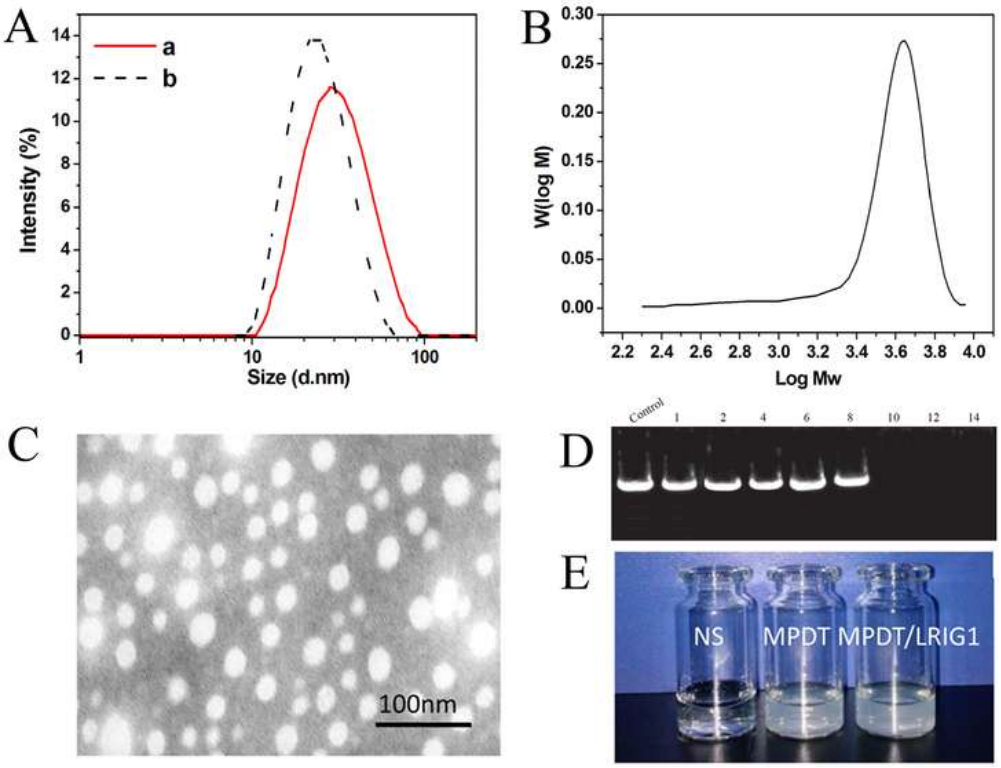

Figure 3 Characterization of micelles. A Size distribution spectrum of MPDT before binding plasmids (a); Size distribution spectrum of MPDT after binding plasmids (b); B The GPC curve of MPEG-PLLA; C TEM image of MPDT after binding plasmids; D Gel retardation assay (PEI25K, DOTAP and MPDT); E Images of NS, MPDT and MPDT/LRIG1 dissolved in water.
61x47mm (300 x 300 DPI)

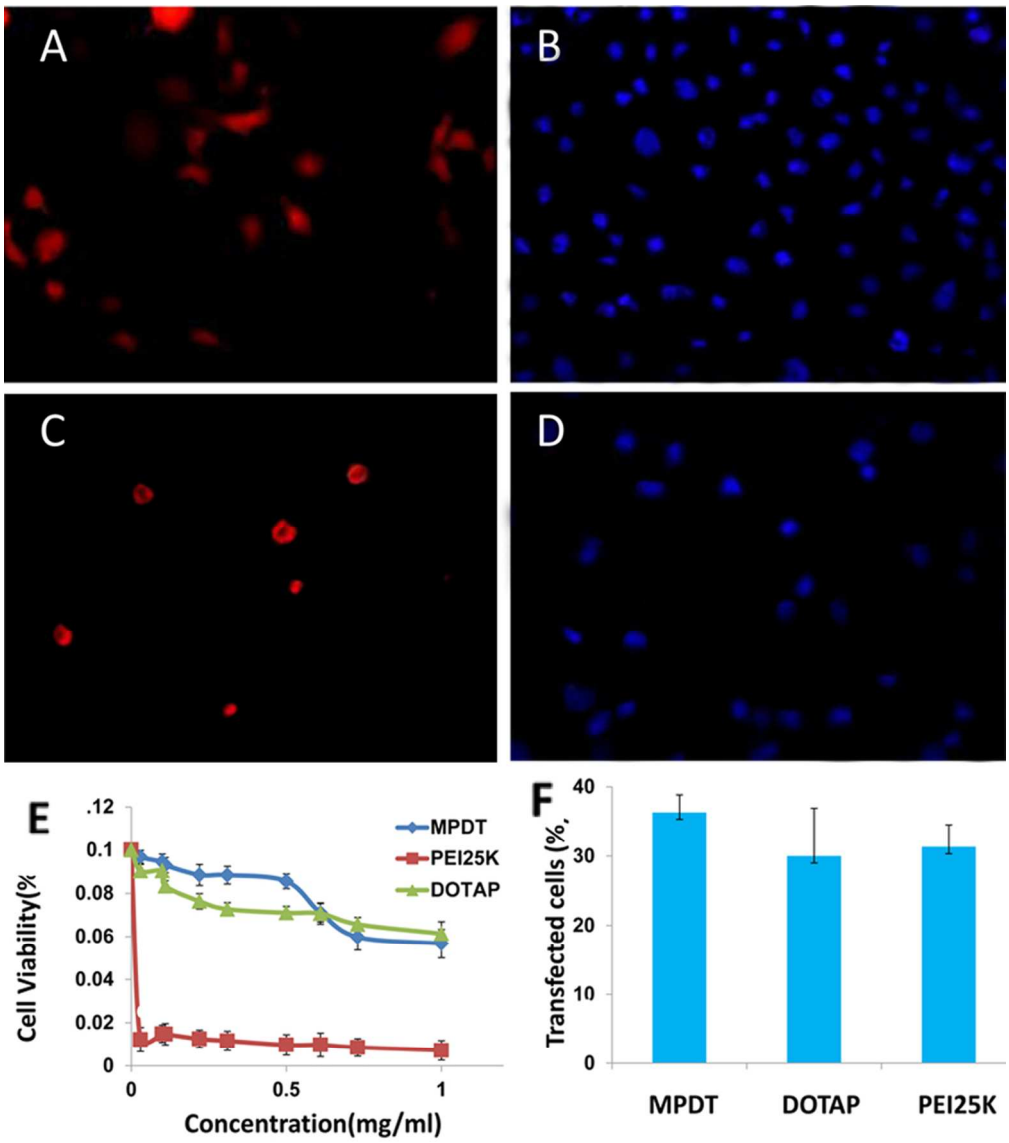

Figure 4 Effects of transfection of 4T1 breast tumor cells in vitro. A Photograph of 4T1 cells transfected by MPDT/pEP in fluorescent light; B Photograph of 4T1 cells transfected by MPDT/pEP in fluorescent light; C Photograph of 4T1 cells transfected by MPDT/ LRIG1 in fluorescent light; D Photograph of 4T1 cells transfected by MPDT/ LRIG1 in fluorescent light; E Cell viability assay (MPDT, DOTAP and PEI25K); F In vitro transfection efficiency of MPDT, DOTAP and PEI25K.
91x104mm (300 x 300 DPI)

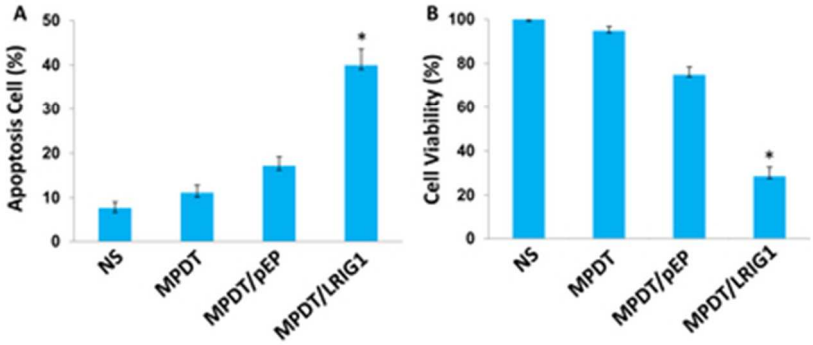

Figure 5 Cytotoxicity studies of MPDT micelles on 4T1 cells. A Apoptosis measured by flow cytometric analysis; B Cytotoxicity evaluation of MPDT micelles on 4T1 cells in vitro by MTT assay. * $P<0.05$.
34x15mm (300 x 300 DPI)

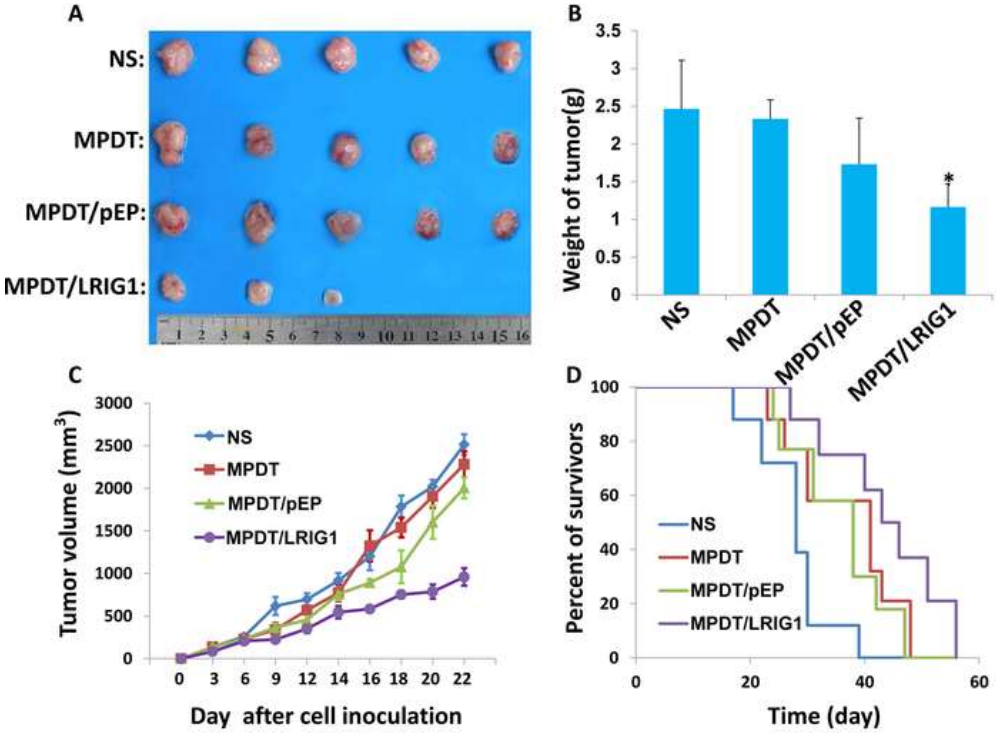

Figure 6 MPDT micelles inhibited growth in a subcutaneous model of 4T1 breast cancer. A Photographs of subcutaneous tissue bearing metastases of 4T1 breast cancer; B Weight of subcutaneous metastases of 4T1 breast carcinoma; C Tumor volume of 4T1 breast carcinoma; D Survival curves of mice. * $P<0.05$.
59x44mm (300 x 300 DPI)

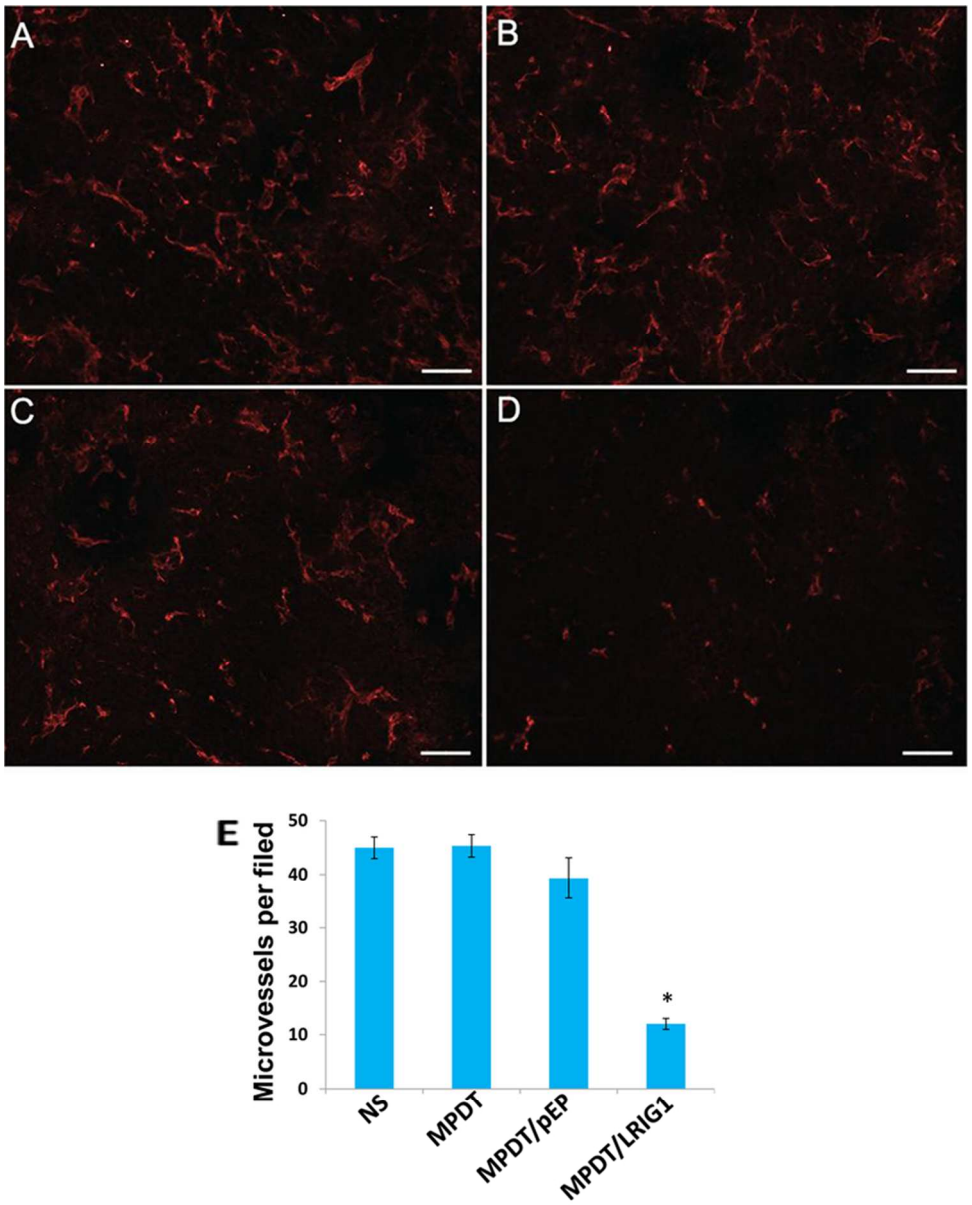

Figure 7 CD31 immunohistochemical staining of subdermal metastases of 4T1 breast carcinoma. A Control group; B MPDT micelle group; C MPDT/pEP complex group; D MPDT/LRIG1 complex group; E The MVD in each group. *P<0.05.
99x123mm (300 x 300 DPI)

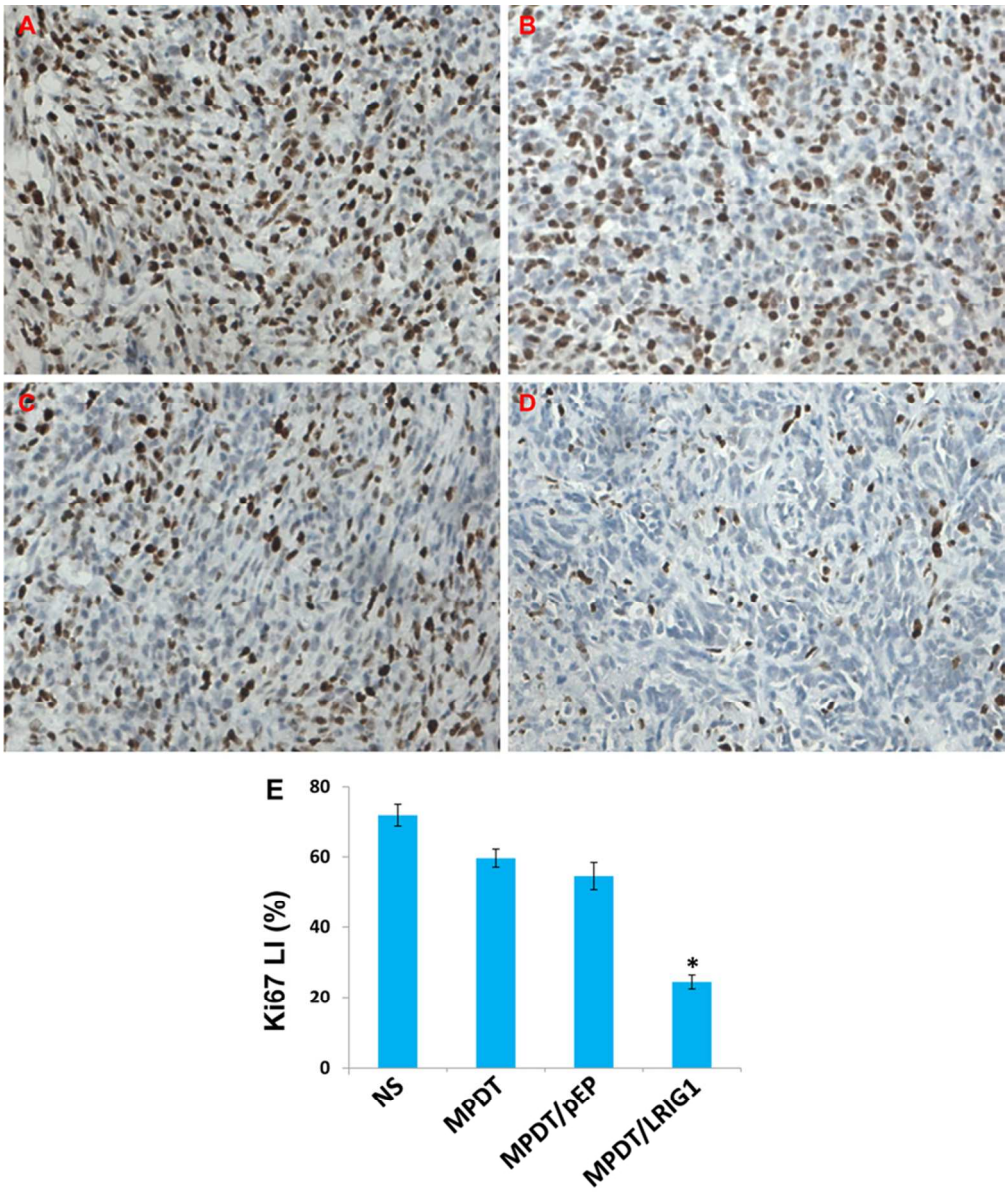

Figure 8 Ki67 immunohistochemical staining of subdermal metastases of 4T1 breast carcinoma. A Control group; B MPDT micelle group; C MPDT/pEP complex group; D MPDT/LRIG1 complex group; E Ki67 LI in each group. *P<0.05.
95x113mm (300 x 300 DPI)